

## STM Studies of GMR Spin Valves

R. D. K. Misra,\* T. Ha\*\*, Y. Kadmon,\*\*\* C. J. Powell, M. D. Stiles, R. D. McMichael,  
and W. F. Egelhoff, Jr.,

National Institute of Standards and Technology  
Gaithersburg, MD 20899

### Abstract

We have investigated the surface roughness and the grain size in giant magnetoresistance (GMR) spin valve multilayers of the general type:  $\text{FeMn/Ni}_{80}\text{Fe}_{20}/\text{Co/Cu/Co/Ni}_{80}\text{Fe}_{20}$  on glass and aluminum oxide substrates by scanning tunneling microscopy (STM). The two substrates give very similar results. These polycrystalline GMR multilayers have a tendency to exhibit larger grain size and increased roughness with increasing thickness of the metal layers. Samples deposited at a low substrate temperature (150 K) exhibit smaller grains and less roughness. Valleys between the dome-shaped individual grains are the dominant form of roughness. This roughness contributes to the ferromagnetic, magnetostatic coupling in these films, an effect termed "orange peel" coupling by Néel. We have calculated the strength of this coupling, based on our STM images, and obtain values generally within about 20% of the experimental values. It appears likely that the ferromagnetic coupling generally attributed to so-called "pinholes" in the Cu when the Cu film thickness is too small is actually "orange peel" coupling caused by these valleys.

### Introduction

In the few years since the giant magnetoresistance (GMR) effect was discovered [1-3], cross-section transmission electron microscopy (TEM) has been used extensively to characterize of GMR structures, [4] but surprisingly little use has been made of scanning tunneling microscopy (STM). Cross-section TEM views a thin-film sample side-on, and presents an image that is in a sense an average over the width of the sample, which is thinned-down to a few tens of nanometers (nm) for TEM. Such images provide useful information about the layering structure in the interior of GMR multilayers. However, additional detail about the film morphology is available from STM, which views a sample surface from above and is not subject to the averaging effect just described. Our purpose in this work is to examine the interior of GMR spin valves by terminating the deposition at various stages of growth and examining the resulting surfaces by STM.

There has been a growing interest [5] in the "orange peel" coupling idea of Néel [6] largely as a result of its apparent manifestation in GMR spin valves [7]. This idea, which is illustrated in Fig. 1, is that if two magnetic films are separated by a nonmagnetic film then any bumps or protrusions in the magnetic films will have magnetic poles on them, and a dipole field will be set up (this model assumes the magnetization is in the plane of the film). If this roughness is conformal (i.e., if the same bumps occur in all three films one above another), then the dipole fields will interact in a manner that tends to produce parallel (or ferromagnetic) alignment in the magnetic films. This means, for example, that if one magnetic film is pinned by

FeMn, and one is unpinned, the hysteresis loop of the unpinned film will be shifted off center from zero field by an amount corresponding to the strength of the interaction.

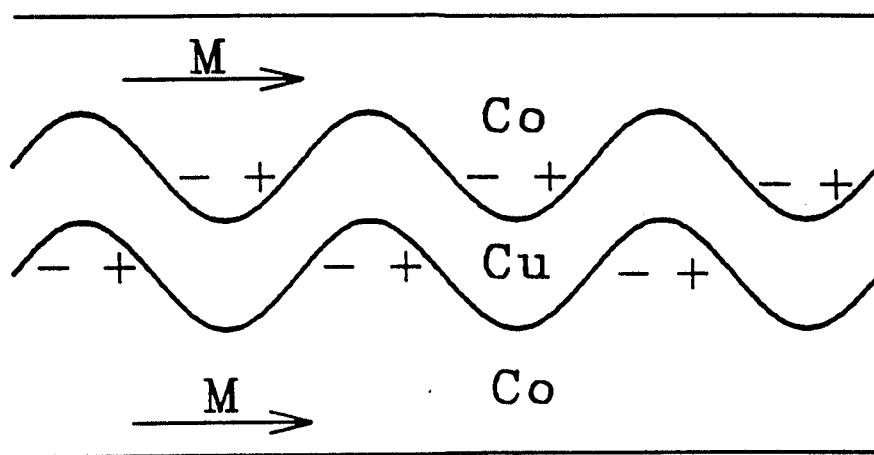


**Figure 1** An illustration to the "orange peel" coupling idea of Néel[6] in which magnetostatic coupling occurs due to the interaction of magnetic poles in a magnetic/nonmagnetic/magnetic structure with conformal roughness.

## Experimental

The two types of substrates used in this work were cover-glass slides and aluminum oxide films on Si wafers. The cover-glass slides and the Si wafers were cleaned ultrasonically, rinsed in distilled water, dried, and installed in the deposition chamber.

It is very important to remove the hydrocarbon contamination on the cover-glass slides (several tenths of a nm of which is accumulated on the glass substrate from exposure to the laboratory air) prior to the deposition of each spin valve in order to achieve the highest GMR values. Samples were Ar<sup>+</sup> sputtered with a neutralized-beam ion gun at a beam voltage of 500 eV until the carbon was removed, as judged by x-ray photoelectron spectroscopy (XPS) in a connected chamber.

A 50 nm film of aluminum oxide was deposited *in situ* on the Si wafers by reactive dc-magnetron sputtering of an metallic Al target in a 2 mTorr 85/15 mixture of Ar/O<sub>2</sub> at a rate of ~0.1 nm/s. The GMR films were deposited by sputtering without further treatment of the aluminum oxide.

The base pressure before depositing a spin valve was typically  $2 \times 10^{-8}$  Torr ( $\sim 10^{-6}$  Pa) of

which ~95% was  $H_2$  and the remainder largely  $H_2O$ . The presence of  $H_2$  during deposition has no apparent effect on spin valve properties unless the partial pressure exceeds  $\sim 10^{-6}$  Torr. The low base pressure is achieved, in part, by depositing a  $\sim 1.5$  nm Ti film on the inside of the deposition chamber from a centrally mounted Ti filament just prior to deposition of each spin valve.

The metal films were deposited by dc-magnetron sputtering in 2 mTorr Ar at a rate of  $\sim 0.1$  nm/s. During deposition the samples are subject to an in-plane field of  $\sim 20$  mT (200 Oe) provided by permanent magnets mounted on either side of the sample on two quartz-crystal-oscillator holders. The magnetoresistance measurements were made *in situ* in the DC mode using a 4-point probe with a  $5\frac{1}{2}$  digit ohm meter under computer control.

The scanning tunneling microscope (STM) is connected to the deposition chamber through a vacuum interlock so that samples could be transferred and investigated in a vacuum of better than  $10^{-7}$  Torr. This vacuum appears to be adequate since we found little change in the roughness and no change at all in the grain size upon brief exposures (e.g., 1 min.) of these samples to air (by opening the STM to air during a scan). All images were recorded with a tunneling current of 0.2 nA with the tip biased at -50 mV with respect to the sample. The tips were prepared from 0.25 mm  $Pt_{90}Ir_{10}$  wire clipped it under tension with a wire cutter. For the STM data discussed here, multiple images were taken at a variety of locations on each sample to ensure that the results were indeed typical of that sample. Care was taken to ensure that the data were not influenced by the use of different tunneling tips. The majority of data was recorded with a single tip, and great effort was devoted to repeated intercomparisons among the samples to ensure that changing tip conditions did not change the main features of the data. This approach is important because the STM image can be a convolution of the sample and tip morphologies. If the features on the sample are sharper than the tip, as could occur in pathological cases, the sample may even image the tip.

## Results and Discussion

The present work was based on a rather common type of spin valve structure  $FeMn/Ni_{80}Fe_{20}/Co/Cu/Co/Ni_{80}Fe_{20}$ , which often achieves a moderate GMR at a rather low coercivity.[6] The top two magnetic films ( $Ni_{80}Fe_{20}$  and Co) are pinned by exchange bias from the FeMn, and the bottom two magnetic films (Co and  $Ni_{80}Fe_{20}$ ) are free to switch at low applied fields (unpinned). The standard sample of this type used as a reference point in the present work is illustrated in Fig. 2. In our work such samples typically give a GMR of 8%, a coercivity of 0.5 mT (5 Oe), and a coupling field of 0.8 mT (8 Oe).[8] These studies will be published separately.[8]

The present studies concentrated on the STM images at the early and middle stages of deposition of films such as those illustrated in Fig. 2. The issues of principle interest in this work lay in two areas. One was that of nucleation and growth in the early stages of deposition, and the other was that of grain size and roughness at the Cu layer, which plays a key role in the GMR effect.

We found it impossible to obtain STM images on our bare substrates, which are highly insulating. After deposition of  $\sim 1$  nm of  $Ni_{80}Fe_{20}$ , images of low quality could be obtained and it seems likely that a partially continuous metal film was present: nevertheless bare regions of the

insulating substrate impaired the quality of the images. After deposition of 2.5 nm of  $\text{Ni}_{80}\text{Fe}_{20}$ , good images could be obtained, but this thickness was found to be too thin for optimum spin valve performance. If the bottom  $\text{Ni}_{80}\text{Fe}_{20}$  film is 2.5 nm thick instead of the optimum value of 5 nm in the type of structure illustrated in Fig. 2, the coupling rises from 0.8 mT to 2 mT (8 Oe to 20 Oe) and the GMR drops from 8% to 6%. [8]

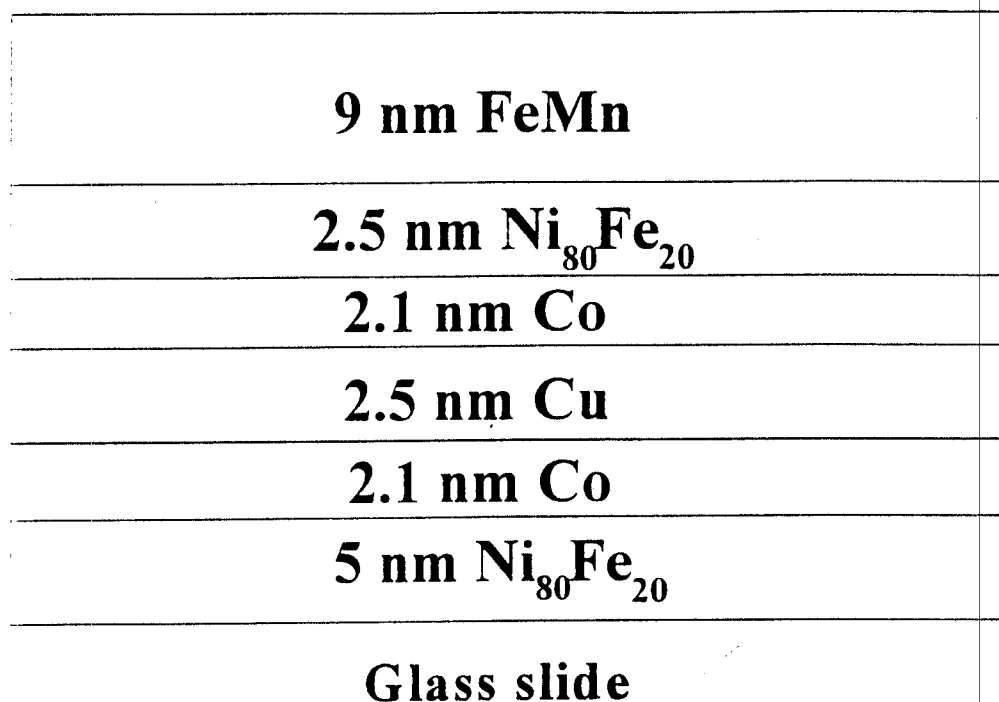
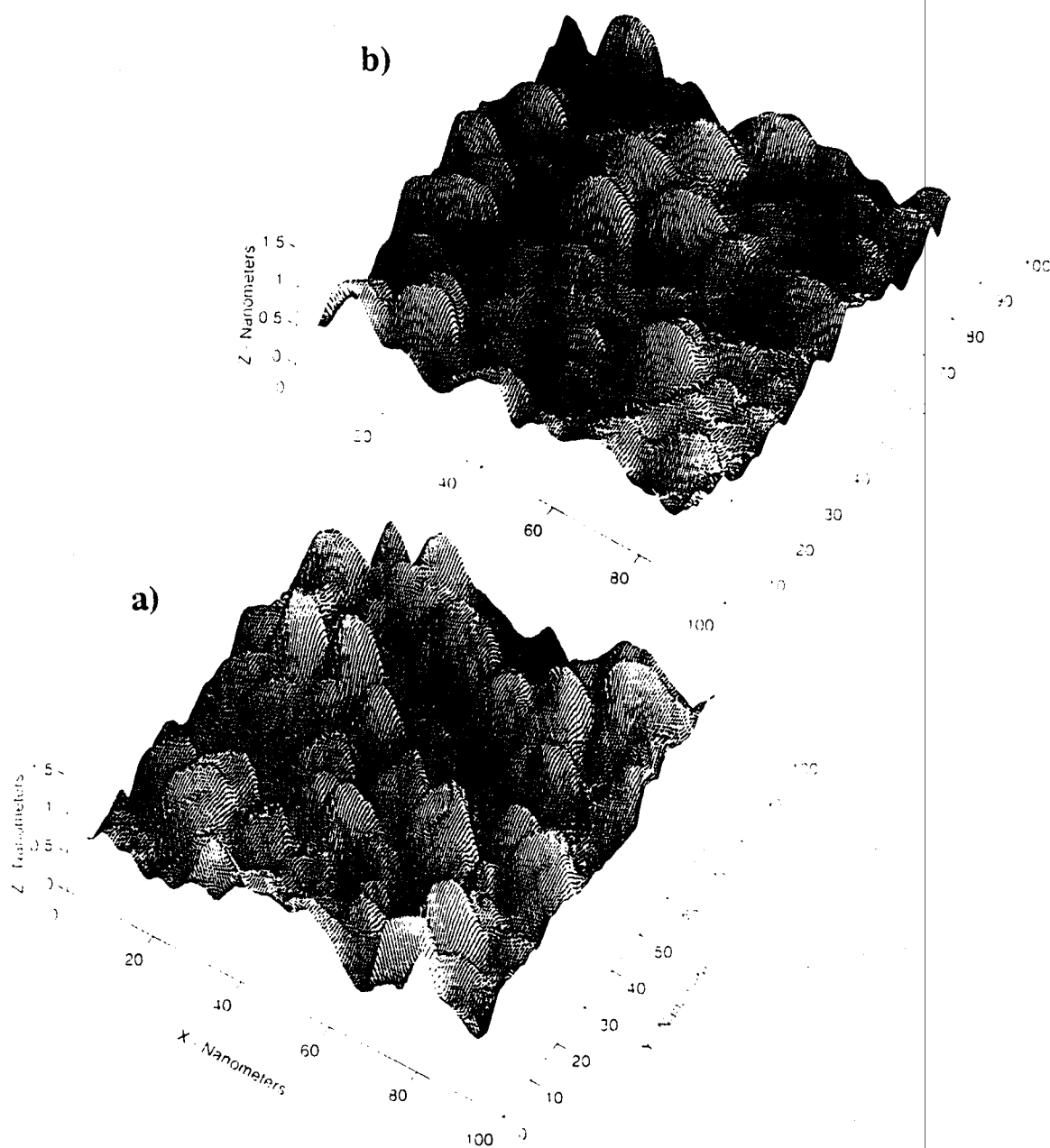


**Figure 2** An illustration of a standard type of spin valve structure on which the present investigations are based.

Figure 3 presents two typical STM images of samples after deposition of the optimum 5 nm of  $\text{Ni}_{80}\text{Fe}_{20}$ . Figure 3a presents the result for deposition at room temperature, and Fig. 3b presents the result for deposition at 150 K followed by warming to room temperature for the STM studies. Deposition at 150 K is of interest because in recent work we have found that the GMR can be increased to 9% or even 10%. [8]

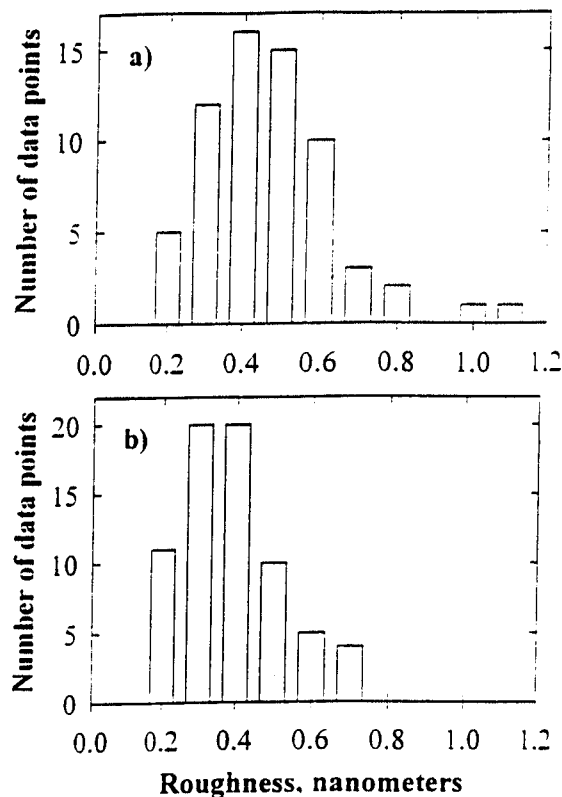
The first thing to note about the images in Fig. 3 is that the vertical scale is 15 times smaller than the horizontal scales. The resulting vertical exaggeration is an important aid in visualizing the surface roughness since these films are actually quite smooth.

The most noticeable difference between these two images is that the  $\text{Ni}_{80}\text{Fe}_{20}$  film deposited at room temperature (RT) may be seen to have somewhat sharper or more pronounced peaks associated with each grain than the  $\text{Ni}_{80}\text{Fe}_{20}$  film deposited at 150 K. However, other differences between these images are not readily apparent by mere visual inspection, and it is very helpful to quantify the images.



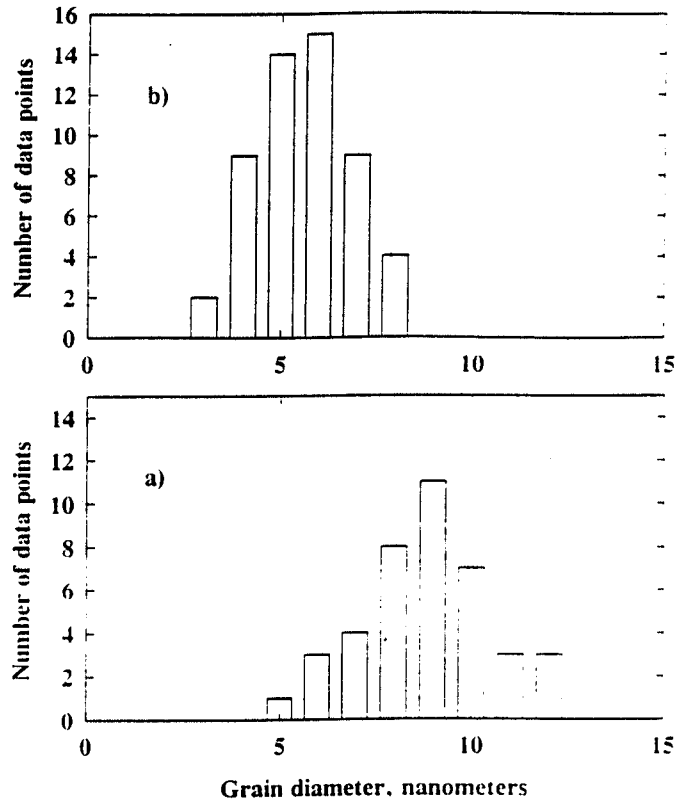
**Figure 3** The STM images of an early stage of deposition of a typical spin valve structure. In a) 5 nm of  $\text{Ni}_{80}\text{Fe}_{20}$  was deposited at room temperature, and in b) 5 nm of  $\text{Ni}_{80}\text{Fe}_{20}$  was deposited at 150 K and the sample warmed to room temperature for the STM studies. The STM is *in situ*, and the samples were in high vacuum continuously.

Figure 4 presents the results of quantifying the surface roughness in images of the type illustrated in Fig. 3 (several locations were imaged on each sample). In this case, the roughness was defined as the difference in height between the maximum at the center of each grain and the depth of an adjacent valley. The depth of the valleys in the positive and negative x and y directions (from the grain center) were counted as four separate data points. This particular definition of roughness seems appropriate for assessing the importance of the "orange peel" coupling illustrated in Fig. 1. A comparison of Figs. 4a and 4b suggests that there is not a great difference between them. The film deposited at RT is only slightly rougher.



**Figure 4** Histogram plots of the surface roughness (defined in the text) for the samples of Fig. 3, where a) corresponds to 5 nm  $\text{Ni}_{80}\text{Fe}_{20}$  deposited at RT and b) to 5 nm  $\text{Ni}_{80}\text{Fe}_{20}$  deposited at 150 K.

Measurements of the average grain diameter, presented in Fig. 5, show major differences between images of the two types of samples. We define the grain diameter as the distance between minima on opposite sides of a grain. Most grains are nearly circular. For those that are elongated, the average of the long and short distances was plotted. The major difference in grain diameter apparent in Fig. 5 is not readily apparent in Fig. 3 because the vertical exaggeration tends to hide the depths of the minima. This shortcoming illustrates the value of quantifying the images.



**Figure 5** Histogram plots of the grain diameter (defined in the text) for the samples of Fig. 3, where a) corresponds to 5 nm  $\text{Ni}_{80}\text{Fe}_{20}$  deposited at RT and b) to 5 nm  $\text{Ni}_{80}\text{Fe}_{20}$  deposited at 150 K.

The smaller average grain size in Fig. 5b compared to Fig. 5a is attributable to less diffusion of deposited atoms at 150 K than at RT. At lower temperatures grains nucleate more closely together on the substrate and thus grain diameters are smaller when a film becomes continuous. Since grain growth in these systems tends to be columnar,[4] the grain size tends to propagate through the layers. Some increase in grain size with increasing film thickness is apparent, particularly in the early stages. Figure 6a illustrates this increase for  $\text{Ni}_{80}\text{Fe}_{20}$  films of different thickness deposited at RT. The two points plotted in Fig. 6a for the 5 nm  $\text{Ni}_{80}\text{Fe}_{20}$  films correspond to the data of Figs 5a and 5b. Each point in Fig. 6 represents the average of the corresponding histogram and the "error" bars represent one standard deviation in the distribution of values in the histogram.

As mentioned above, the coupling strength increases sharply if the bottom  $\text{Ni}_{80}\text{Fe}_{20}$  layer in a spin valve of the type illustrated in Fig. 2 is 2.5 nm thick rather than the optimum value of 5 nm. From the data of Fig. 6, one can infer that this increase may be attributed to the smaller grain size. The surface roughness is rather similar for the 2.5 and 5 nm thicknesses of  $\text{Ni}_{80}\text{Fe}_{20}$  for RT deposition, as seen in Fig. 6b. However, as seen in Fig. 6a, the grain size is significantly smaller at 2.5 nm  $\text{Ni}_{80}\text{Fe}_{20}$ , and thus there is a higher density of valleys. According to the Néel model, the greater the density of the waviness (illustrated in Fig. 1), the greater will be the

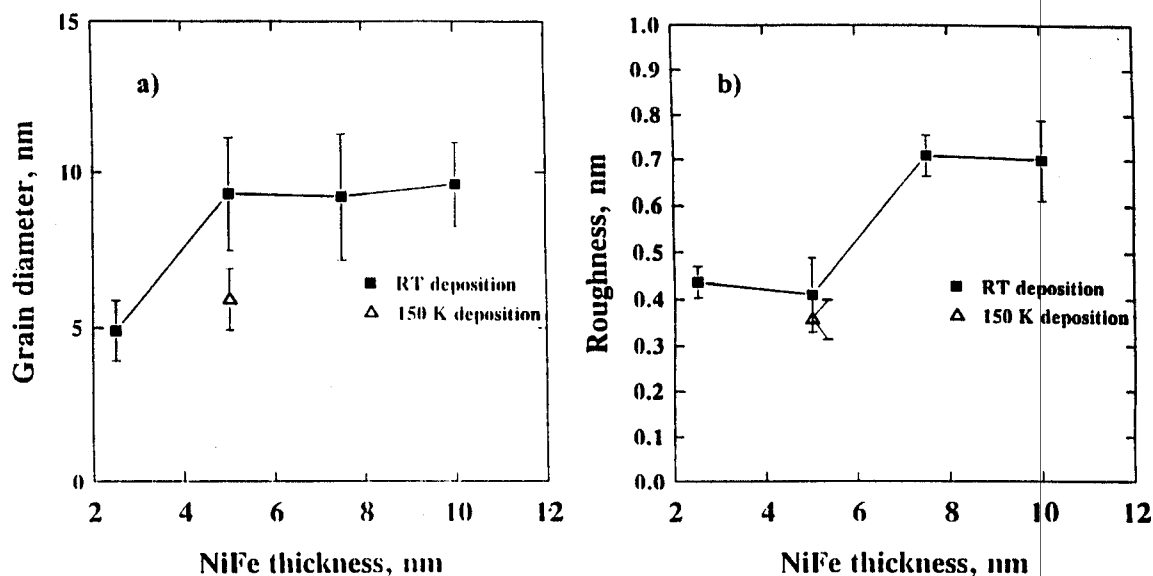


**Figure 6** Plots of a) the grain diameter and b) the surface roughness (see text for definitions) versus  $\text{Ni}_{80}\text{Fe}_{20}$  thickness. The "error" bars represent one standard deviation in the distribution of observed values. The data for the 5 nm  $\text{Ni}_{80}\text{Fe}_{20}$  film correspond to the samples of Fig. 3.

coupling strength, all other things being equal. In the present structures, the valleys between grains are the only prominent form of waviness, and it seems reasonable to attribute the observed magnetostatic coupling to the effects of roughness.

In fact, we have calculated the magnetostatic coupling strength using our STM images and the values obtained are generally within about 20% of the observed values. Several assumptions are made in these calculations. It is assumed that the roughness is conformal, as in Fig. 1, so that an STM image taken after deposition of Cu is representative of both the Co/Cu and the Cu/Co interfaces. It is also assumed that the magnetization is rigidly in-plane right up to the interfaces. In reality, the demagnetizing field will tend to twist the magnetization slightly into parallel alignment with the interface. This twisting is probably responsible for the calculated values tending to be higher than the experimental ones. The calculation is performed by using the slope of the interface to determine the density of magnetic poles, and then by making a simple double sum (of the Coulomb interaction) over the top and bottom poles to get the coupling energy.[9]

Another example of the effect of the grain diameter on the coupling strength may be found in the 150 K deposition data of Fig. 6. The roughness is not very different from the value for RT deposition, but the grain size is significantly smaller for 150 K deposition. The observed coupling strength when the entire spin valve was deposited at 150 K was 1.2 - 1.3 mT (12-13



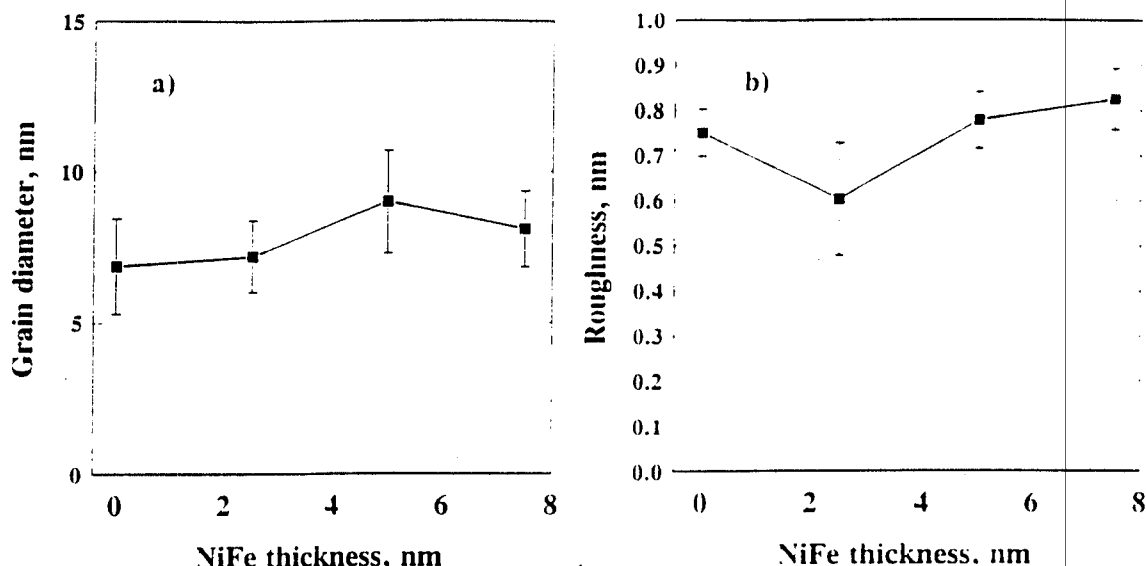


**Figure 7** Plots of a) the grain diameter and b) the surface roughness (see text for definitions) versus  $\text{Ni}_{80}\text{Fe}_{20}$  thickness for spin valves in which deposition was terminated after Cu deposition (see Fig. 2). The "error" bars represent one standard deviation in the distribution observed values. All depositions were at RT. The vertical scales are the same as in Fig. 6 to facilitate comparison.

Oe), or 50% larger than for RT deposition.[8] This increase may be attributed to the increased density of valleys.

Figure 7 presents STM data similar to that of Fig. 6, except that, after deposition of the  $\text{Ni}_{80}\text{Fe}_{20}$ , 2.1 nm Co and 2.5 nm Cu (illustrated in Fig. 2) were also deposited. By comparing Figs. 6 and 7, some insight can be obtained into the evolution of grain size and roughness during film growth. The most noticeable effect is that the plots are somewhat flatter in Fig. 7 than in Fig. 6. For example, the increase in grain diameter in Fig. 7a in going from 2.5 nm to 5 nm of  $\text{Ni}_{80}\text{Fe}_{20}$  is smaller than that in Fig. 6a. The reason for this observation is that the most rapid change in grain size generally occurs in the early stages of film deposition. In Fig. 6, the images are recorded after  $\text{Ni}_{80}\text{Fe}_{20}$  deposition, but in Fig. 7a the images are recorded after  $\text{Ni}_{80}\text{Fe}_{20}$ , Co, and Cu deposition so the film is thicker. Although the increase in grain diameter in Fig. 7a in going from  $\text{Ni}_{80}\text{Fe}_{20}$  thicknesses of 0 to 2.5 to 5 nm is rather modest, there is a more pronounced decrease in coupling strength from >5 mT (>50 Oe) to 2 mT (20 Oe) to <1 mT (<10 Oe), respectively.[8] This nonlinear dependence of coupling strength on the density of valleys is expected on the basis of Fig. 1 since the interaction is dipolar.

No evidence was found in the present studies for the much discussed "pinholes" that are often invoked to explain the strong ferromagnetic coupling generally observed in GMR structures when the Cu layer is too thin. The roughness in Figs. 6b and 7b for a 5 nm  $\text{Ni}_{80}\text{Fe}_{20}$

film is about 0.7 nm whereas the Cu film must be thinner than about 1.9 nm in our spin valves for the coupling to be so strong that it eliminates any GMR. This observation makes true pinholes in the Cu (direct contact between the two Co films) seem unlikely in our structures. Furthermore, no depressions at all were observed on the Cu that were as deep as 1.9 nm. Finally, the roughness in our structures seems likely to be conformal (as sketched in Fig. 1). Conformal roughness is widely observed in TEM studies of GMR structures.[4] and the fact that the roughness is very similar in Figs. 6b and 7b for a 5 nm  $\text{Ni}_{80}\text{Fe}_{20}$  thickness is probably the result of conformal roughness. Therefore, it seems that rather than attributing strong ferromagnetic coupling to pinholes in the Cu, it would be more plausible to attribute it to the "orange peel" coupling idea of Néel. In our calculations we find that the coupling strength rises steeply as the Cu thickness decreases below 2 nm, varying roughly as the inverse square of the Cu thickness, as would be expected for a dipolar interaction.

All other things being equal, the use of thinner Cu films tends to produce a larger GMR effect because of the increased proportion of conduction electrons crossing the Cu layer. However, as the above discussion makes clear, roughness in the form of valleys between grains in these polycrystalline films seems to be the major factor limiting how thin the Cu can be made in practice. This situation suggests that larger GMR values may be attained in the future if deposition methods can be found to suppress the depths of valleys.

## Conclusions

The major conclusions of this work may be summarized as follows.

- 1) STM observations of GMR spin valves show that valleys between grains are the dominant form of roughness.
- 2) These valleys have about the right depth and occur in about the right concentration to explain the observed magnetostatic coupling using the "orange peel" coupling idea of Néel.
- 3) The deposition of spin valve structures at 150 K produces smaller grain size and similar values of the roughness. The resulting greater density of valleys produces increased coupling strength.
- 4) Additional increases in GMR may be possible if deposition methods can be found to reduce the depth of these valleys further so that thinner Cu films may be used.

\*Present address: Defense Metallurgical Institute, Hyderabad, India

\*\*Present address: 5248 Signal Hill Rd., Orlando, FL 32808

\*\*\*Present address: NRCN, Beer-Sheva, Israel

## Acknowledgements

The authors would like to acknowledge useful conversations with Drs. J. M. Daughton, S. S. P. Parkin, and V. S. Speriosu. This work has been supported in part (W.F.E. and R.D.McM.) by the NIST Advanced Technology Program.

## References

- [1] E. Velu, C. Dupas, D. Renard, J. P. Renard, and J. Seiden, *Phys. Rev. B* 37, 668 (1988)
- [2] G. Binasch, P. Grunberg, F. S. Sauerbach, and W. Zinn, *Phys. Rev. B* 39, 4828 (1989)
- [3] M. N. Baibich, J. M. Broto, A. Fert, F. Nguyen van Dau, F. Petroff, P. Etienne, G. Creuzet, A. Friederich, and J. Chazelas, *Phys. Rev. Lett.* 61, 2472 (1988)
- [4] S. S. P. Parkin, Z. G. Li, and D. J. Smith, *Appl. Phys. Lett.* 58, 2710 (1991); R. J. Highmore, W. C. Shih, R. E. Somekh, J. E. Evetts, *J. Mag. Mag. Mat.* 116, 249 (1992); A. R. Modak, D. J. Smith, and S. S. P. Parkin, *Phys. Rev. B* 50, 4232 (1994); T. Shinjo, *Surface Sci. Rep.* 12, 49 (1991); R. F. C. Farrow, R. F. Marks, G. R. Harp, D. Weller, T. A. Rabedeau, M. F. Toney, and S. S. P. Parkin, *Mat. Sci. Eng. R11*, 155 (1993)
- [5] G. S. Almasi and K. Y. Ahn, *J. Appl. Phys.* 41, 1258 (1970); A. Layadi and J. O. Artman, *J. Mag. Mag. Mat.* 92, 143 (1990); A. Layadi, J. O. Artman, R. A. Hoffman, C. L. Jensen, D. A. Saunders, and B. O. Hall, *J. Appl. Phys.* 67, 4451 (1990); H. O. Gupta, H. Niedoba, L. J. Heyderman, I. Tomas, I. B. Puchalska, and C. Sella, *J. Appl. Phys.* 69, 4529 (1991); E. W. Hill, J. P. Li, and J. K. Birtwistle, *J. Appl. Phys.* 69, 4526 (1991); R. P. Erickson and J. R. Cullen, *J. Appl. Phys.* 73, 5981 (1993); M. R. Parker, S. Hossain, D. Seale, J. A. Barnard, M. Tan, and H. Fujiwara, *IEEE Trans. Mag.* 30, 358 (1994); D. Altbir, M. Kiwi, R. Ramirez, and I. K. Schuller, to be published.
- [6] L. Néel, *Comp. Rend. Acad. Sci. (France)* 255, 1545 (1962) and 255, 1676 (1962); J.-C. Bruyère, O. Massenet, R. Montmory, and L. Néel, *Comp. Rend. Acad. Sci. (France)* 258, 841 (1964) and 258, 1423 (1964).
- [7] V. S. Speriosu, B. Dieny, P. Humbert, B. A. Gurney, and H. Lefakis, *Phys. Rev. B* 44, 5358 (1991); B. Dieny, V. S. Speriosu, S. S. P. Parkin, B. A. Gurney, D. R. Wilhoit, and D. Mauri, *Phys. Rev. B* 43, 1297 (1991); C. Meny, J. P. Jay, P. Panissod, P. Humbert, V. S. Speriosu, H. Lefakis, J. P. Nozieres, and B. A. Gurney, *Mat. Res. Soc. Symp. Proc.* 313, 289 (1993); and B. Dieny, *J. Mag. Mag. Mat.* 136, 335 (1994)
- [8] W. F. Egelhoff, Jr., R. D. K. Misra, Ha. Y. Kadmon, C. J. Powell, M. D. Stiles, R. D. McMichael, L. H. Bennett, C.-L. Lin, J. M. Sivertsen, and J. H. Judy, to be published
- [9] W. F. Egelhoff, Jr. and Y. Kadmon, to be published